Thermochemical properties of rare earth complexes with salicylic acid

Xu-Wu Yang [a,∗], Wu-Juan Sun [b], Cong-Yu Ke [c],
Hang-Guo Zhang [a], Xiao-Yan Wang [a], Sheng-Li Gao [a]

[a] *Shaanxi Key Laboratory of Physico-Inorganic Chemistry, Department of Chemistry,*
Northwest University, Xi'an, Shaanxi 710069, PR China
[b] *College of Chemistry and Environment Science, Shaanxi University of Technology, Hanzhong, Shaanxi 723001, PR China*
[c] *Institute of Modern Separation Science, Northwest University, Xi'an 710069, PR China*

Abstract

Fourteen rare earth complexes with salicylic acid $RE(HSal)_3 \cdot nH_2O$ ($HSal = C_7H_5O_3$; $RE = La–Sm$, $n = 2$; $RE = Eu–Lu$, $n = 1$) were synthesized and characterized by elemental analysis, and their thermal decomposition mechanism were studied with TG–DTG technology. The constant-volume combustion energies of complexes, $\Delta_c U$, were determined by a precise rotating-bomb calorimeter at 298.15 K. Their standard molar enthalpies of combustion, $\Delta_c H_m^\circ$, and standard molar enthalpies of formation, $\Delta_f H_m^\circ$, were calculated.

1. Introduction

Nowadays great attention has been paid to the lanthanide aromatic carboxylates owing to their novel structures and potential applications in material sciences as superconductors, magnetic materials, and luminescent probes [1–5]. Moreover, they are a kind of potential luminescent materials for further application. The luminescence, stability constants, and other properties of some lanthanide complexes with salicylic acid have been reported in literatures [6–8]. However, thermochemistry of lanthanide complexes with salicylic acid has not been systematically investigated. In this paper, thermal decompositional mechanisms of 14 complexes were studied according to TG–DTG curves. The constant-volume combustion energies of 14 complexes were determined by a precise rotating-bomb calorimeter at 298.15 K and their standard molar enthalpies of combustion and standard molar enthalpies of formation were calculated on the basis of the constant-volume combustion energies of complexes.

2. Experimental

2.1. Materials

Lanthanide chloride hydrate, $RECl_3 \cdot nH_2O$ ($RE = La–Lu$, except Pm, $n = 3–4$) were prepared according to Ref. [9], their purity was more than 99.9%. Salicylic acid (made in Guangzhou Chemical Reagent Company) and sodium hydroxide (made in Xi'an Chemical Reagent Company) were of analytical grade.

Fourteen complexes were prepared according to Ref. [10]. The purity of the compounds was 99.9%, checked by LC-10A type high performance liquid chromatography analyzer (made in Japan), adopting the solvent DMF, the mobile phase DMF-H_2O and the reversed phase C_{18} column.

2.2. Experimental equipment and conditions

The C and H contents were measured by a Vario EL III CHNOS elemental analyzer made in Germany. The rare earth ion was determined by EDTA volumetric analysis. All TG–DTG tests were performed with a Perkin-Elmer thermogravimetric instrument, the purge gas was nitrogen flow of 60 ml min^{-1}. A heating rate of 10 °C min^{-1} was adopted, with samples weighing

---

∗ Corresponding author. Tel.: +86 29 88302054; fax: +86 29 88303798.
E-mail address: yangxuwu@nwu.edu.cn (X.-W. Yang).

about 4–8 mg, the intermediate and final products of the thermal decomposition of the complexes were identified by IR spectra and XRD as well.

The constant-volume combustion energies of the compounds were determined by a precise rotating-bomb calorimeter (RBC-type II). The main experimental procedures were described previously [11]. The initial temperature was regulated to $(25.0000 \pm 0.0005)\,°C$, and the initial oxygen pressure was 2.5 MPa. The correct value of the heat exchange was calculated by mean of the following equation according to the literature [12]:

$$\varsigma = \left(\frac{V_n - V_0}{\theta_n - \theta_0}\right)\left(\frac{T_0 - T_n}{2} + \sum_{i=1}^{n-1}T_i - n\theta_n\right) + nV_n$$

where ς (K) denotes the correction value of the heat exchange; n, the number of readings for the main (or reaction) stage; V_n (K min^{-1}) and V_0 (K min^{-1}), the temperature drift rates in the final and initial stages, respectively (V is positive when the temperature decrease); θ_n (K) and θ_0 (K), the average temperature of the calorimeter during the final and initial stages, respectively; T_0 (K), the last reading of the initial stage; T_n (K), the first reading of the final stage; $\sum_{i=1}^{n-1}T_i$, the sum of all the temperature readings, except for the last one, of the main stage; $(V_n - V_0)/(\theta_n - \theta_0)$, a constant relative to the calorimeter performance.

The energy equivalent of the calorimeter was calibrated with benzoic acid of 99.999% purity, which has an isothermal heat of combustion of $-26{,}434\,J\,g^{-1}$ at 25 °C, the calibrated experimental results with an uncertainty 4.18×10^{-4} was $17775.09 \pm 7.43\,J\,K^{-1}$.

After the experiment was over, the final products of the combustion reaction were analyzed [12]. The gases formed in the combustion were collected in a gas-collecting bag. The volume was measured by a gas meter, which was fitted between the bag and the bomb. The gaseous carbon dioxide produced in the combustion was absorbed by a weighted absorption tube containing alkali asbestos. The amount of CO_2 was determined through the weight increase of the tube after absorbing the carbon dioxide. The amount of CO_2 dissolved in the final solution was ignored. Four absorption tubes were connected in series for the vapor measurement. The first was filled with P_4O_{10} and $CaCl_2$ (anhydrous) to absorb the water vapor contained in the gas, the second was filled with alkali asbestos to absorb the CO_2, and the third was full of the solid P_4O_{10} and $CaCl_2$ (anhydrous) to absorb the water vapor formed in the determination. The fittings and interior surfaces of the bomb were first washed three times using distilled water; after this, the bomb solution (including the washing solution) was completely transferred to a conical bottle and heated to boiling to remove the small amount of CO_2 dissolved in the bomb solution. Since the crucible in the rotating-bomb was attached to the support, the final solid products were left in the crucible at the end of the experiment. The results from the IR spectra, XRD, chemical, and elementary analyses showed that the final solid product was monoclinic rare earth sesquioxide. Analyses of the combustion products indi-

Table 1
Analytical results related to the composition of the complexes

Complex	w (found) (%) (w (calculated) (%))			Yield (%)
	RE	C	H	
La(HSal)$_3$·2H$_2$O	23.67 (23.69)	43.17 (42.98)	2.98 (3.24)	93
Ce(HSal)$_3$·2H$_2$O	23.47 (23.85)	42.74 (42.90)	3.01 (3.23)	92
Pr(HSal)$_3$·2H$_2$O	23.61 (23.95)	42.98 (42.84)	3.45 (3.23)	90
Nd(HSal)$_3$·2H$_2$O	24.68 (24.38)	42.35 (42.60)	3.17 (3.21)	89
Sm(HSal)$_3$·2H$_2$O	24.76 (25.16)	42.40 (42.16)	2.86 (3.18)	90
Eu(HSal)$_3$·H$_2$O	26.19 (26.15)	43.75 (43.38)	2.75 (2.95)	90
Gd(HSal)$_3$·H$_2$O	26.58 (26.81)	43.42 (42.96)	3.03 (2.90)	83
Tb(HSal)$_3$·H$_2$O	26.61 (27.01)	42.97 (42.84)	2.80 (2.89)	74
Dy(HSal)$_3$·H$_2$O	27.07 (27.46)	42.76 (42.58)	2.95 (2.87)	61
Ho(HSal)$_3$·H$_2$O	27.98 (27.75)	42.23 (42.41)	2.65 (2.86)	44
Er(HSal)$_3$·H$_2$O	28.50 (28.04)	42.55 (42.24)	2.99 (2.85)	57
Tm(HSal)$_3$·H$_2$O	28.64 (28.23)	42.36 (42.12)	2.83 (2.84)	60
Yb(HSal)$_3$·H$_2$O	29.01 (28.72)	41.63 (41.84)	2.74 (2.82)	44
Lu(HSal)$_3$·H$_2$O	28.99 (28.96)	41.82 (41.70)	2.94 (2.81)	40

cated that the compound was combusted to CO_2 (g), H_2O (l), and RE_2O_3 (s) (RE = La, Pr–Lu) (the final solid product of Ce compound is CeO_2) under excess oxygen. The amount of CO in the final gas phase can be ignored. The analytical results of the final products showed that the combustion reactions were complete.

3. Results and discussion

3.1. Composition of complexes

The analytical results of the composition of these complexes are presented in Table 1.

3.2. Thermostabilities of the solid complexes

The thermal decompositional intermediates products, final decompositional products and the percentage of residue in every step of 14 complexes with salicylic acid are presented in Table 4 (see Appendix A). The thermal decompositional procedure of La and Ce complexes are shown in Figs. 1 and 2. As for other complexes, the TG–DTG figures are similar with La complex or Ce complex. As shown in TG–DTG figures, the thermal decom-
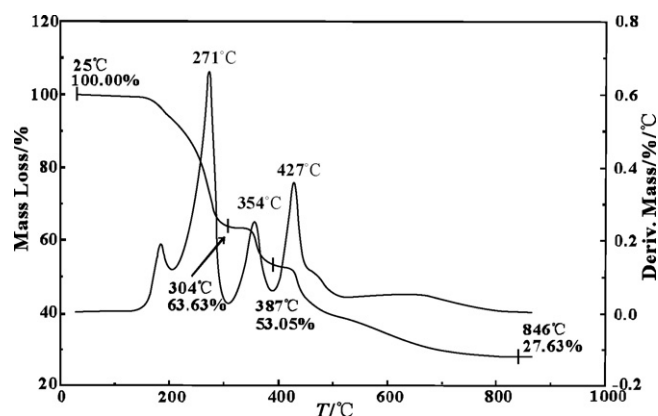

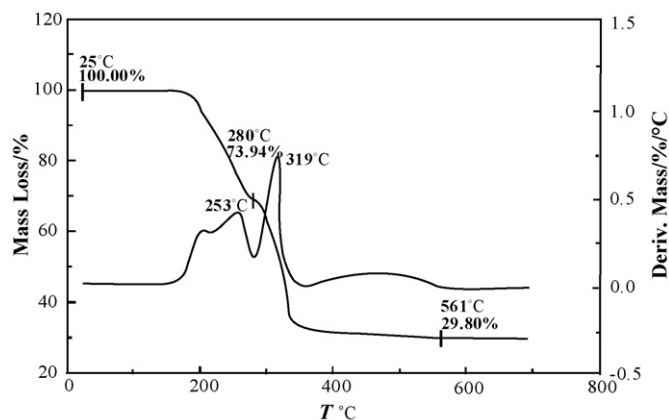
Fig. 1. TG–DTG curves of La complex.

Fig. 2. TG–DTG curves of Ce complex.

position process of Ce, Tm, Yb and Lu complexes with salicylic acid takes two steps, while that of the other complexes falls into three steps. However, the first stage intermediate products and the final decompositional products of all complexes are similar, which are $(1/2)Ln(C_6H_4OHCOO)_3\cdot(1/4)Ln_2O_2CO_3$ (Ce is $(1/2)Ce(C_6H_4OHCOO)_3\cdot(1/2)CeOCO_3$) and $(1/2)Ln_2O_3$ (Ce is the CeO_2), respectively.

It is partial decomposition of the complexes in the first two stages, and the products are mixture of the complexes and basic carbonates. It can be seen from the TG–DTG curves of complexes that the temperature of first stage decomposition is in the range of 25–385 °C, and from La to Dy, all the complexes have the dehydration peaks, but the dehydration peaks in heavy rare earth complexes are not clear. The reason is probably that the lanthanide atomic radius shrinks, so the metal ion with big radius can exist stably after dehydrating, while the heavy rare earth complex with small radius dehydrates and decomposes at the same time. Therefore, it can be concluded that from Ho to Lu hydrated heavy rare earth complexes are less stable than light and middle rare earth complexes. Perhaps just because of this, the complexes of salicylic acid from Tm to Lu completely decompose to rare earth oxides in two stages. The second stage decomposition is complete and clear, and the temperature of it is in the range of 300–428 °C. The decompositional intermediate product is $(1/3)Ln(C_6H_4OHCOO)_3\cdot1/3Ln_2O_2CO_3$ (Ln stands for the other rare earth elements except Ce, Tm, Yb and Lu). The process of third stage decomposition is complex and has many unstable intermediate products. Because the TG curves' stages are not very clear, they are classified into one stage. And the final decompositional product is Ln_2O_3 (Ce complex is CeO_2). The temperature of Pr_2O_3 formation is the highest. As for Ce complex of salicylic acid, probably because the intermediate product of Ce(III) converts into Ce(IV), its decompositional process has two stages. The first stage is similar to that of other complexes, but in the second stage it directly decomposes to CeO_2. The temperature of CeO_2 formation is lowest.

3.3. Constant-volume combustion energies of the complexes

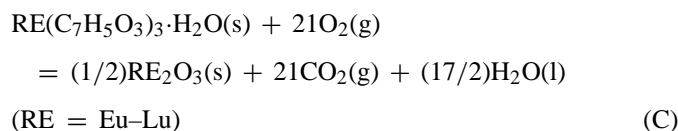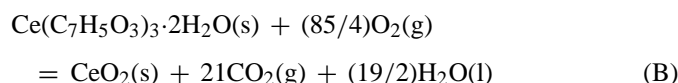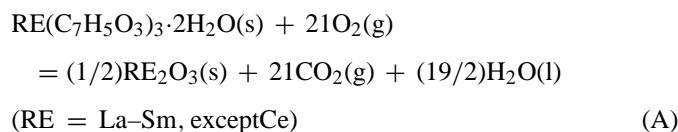The methods of determination and calculation of the constant-volume combustion energies for complexes are the same as for the calibration of the calorimeter with benzoic acid. The values are calculated by means of the following equation:

$$\Delta_c U = \frac{W\Delta T - aG - 5.97b}{m} \tag{1}$$

where $\Delta_c U$ (complexes, s) denotes the constant-volume combustion energy of the complexes (in $J\,g^{-1}$), W the energy equivalent of the rotating-bomb calorimeter (in $J\,K^{-1}$), a is the length of the actual Ni–Cr wire consumed (in cm). G is the combustion enthalpy of Ni–Cr wire for ignition ($0.9\,J\,cm^{-1}$), $5.97\,J\,cm^{-3}$ the formation enthalpy and solution enthalpy of acid corresponding to $1\,cm^3$ of $0.1000\,mol\,dm^{-3}$ NaOH, b the volume (in cm^3) of consumed $0.1000\,mol\,dm^{-3}$ NaOH and ΔT is the correct value of the temperature rise. m is the mass (in g) of the complex. The constant-volume combustion energy of each complex is repetitively determined six times. The experimental results of the combustion energies of the La, Ce, Pr, Nd, Sm, Eu and Gd complexes can be seen in Ref. [13], and that of the Tb, Dy, Ho, Er, Tm, Yb and Lu complexes.

3.4. Standard molar combustion enthalpies of the complexes

The standard molar combustion enthalpies of the complexes, $\Delta_c H_m^\circ$, refer to the combustion enthalpy changes of the following ideal combustion reaction at 298.15 K and 101.325 kPa.

$$RE(C_7H_5O_3)_3\cdot2H_2O(s) + 21O_2(g)$$
$$= (1/2)RE_2O_3(s) + 21CO_2(g) + (19/2)H_2O(l)$$
$$(RE = La\text{–}Sm, exceptCe) \tag{A}$$

$$Ce(C_7H_5O_3)_3\cdot2H_2O(s) + (85/4)O_2(g)$$
$$= CeO_2(s) + 21CO_2(g) + (19/2)H_2O(l) \tag{B}$$

$$RE(C_7H_5O_3)_3\cdot H_2O(s) + 21O_2(g)$$
$$= (1/2)RE_2O_3(s) + 21CO_2(g) + (17/2)H_2O(l)$$
$$(RE = Eu\text{–}Lu) \tag{C}$$

The standard molar combustion enthalpies of the complexes are calculated by the following equations:

$$\Delta_c H_m^\circ = \Delta_c U + \Delta nRT \tag{2}$$

$$\Delta n = n_g(\text{products}) - n_g(\text{reactants}) \tag{3}$$

where n_g is the total amount in mole of gases present as products or as reactants, $R = 8.314\,J\,mol^{-1}$, $T = 298.15\,K$. The results of the calculation are given in Table 3.

3.5. Standard molar enthalpies of formation for the complexes

The standard molar enthalpies of formation of the compounds, $\Delta_f H_m^\circ$, are calculated by Hess's law according to the

thermochemical equations (4)–(6), respectively.

$$\Delta_f H_m^\circ (RE(C_7H_5O_3)_3 \cdot 2H_2O, \text{ s})$$

$$= \left[\frac{1}{2} \Delta_f H_m^\circ (RE_2O_3, \text{ s}) + 21\Delta_f H_m^\circ (CO_2, \text{ g}) \right.$$

$$\left. + \frac{19}{2} \Delta_f H_m^\circ (H_2O, \text{ l}) \right] - \Delta_c H_m^\circ (RE(C_7H_5O_3)_3 \cdot 2H_2O, \text{ s})$$

$$(RE = La\text{–}Sm, \text{ except Ce}) \tag{4}$$

$$\Delta_f H_m^\circ (Ce(C_7H_5O_3)_3 \cdot 2H_2O, \text{ s})$$

$$= \left[\frac{1}{2} \Delta_f H_m^\circ (CeO_2, \text{ s}) + 21\Delta_f H_m^\circ (CO_2, \text{ g}) \right.$$

$$\left. + \frac{19}{2} \Delta_f H_m^\circ (H_2O, \text{ l}) \right] - \Delta_c H_m^\circ (Ce(C_7H_5O_3)_3 \cdot 2H_2O, \text{ s})$$

$$\tag{5}$$

$$\Delta_f H_m^\circ [RE(C_7H_5O_3)_3 \cdot H_2O, \text{ s}]$$

$$= \left[\frac{1}{2} \Delta_f H_m^\circ (RE_2O_3, \text{ s}) + 21\Delta_f H_m^\circ (CO_2, \text{ g}) \right.$$

$$\left. + \frac{17}{2} \Delta_f H_m^\circ (H_2O, \text{ l}) \right] - \Delta_c H_m^\circ [RE(C_7H_5O_3)_3 \cdot H_2O, \text{ s}]$$

$$(RE = Eu\text{–}Lu) \tag{6}$$

The standard molar enthalpies of formation of the rare earth oxide, H_2O (l) and CO_2 (g) [14,15] were listed in Table 2. The results of the calculations are also listed in Table 3.

$\Delta_c H_m^\circ$, $\Delta_f H_m^\circ$ of the complexes are plotted against the atomic numbers of the elements in the lanthanide series, as shown in Fig. 3. The curve shows the "quadripartite effect" of rare earth, suggesting that a certain amount of covalence is present in the chemical bonds between RE^{3+} and ligand, which is caused by the incomplete shield of $5s^2 5p^6$ orbital to 4f electrons. The experimental result is in agreement with the Nephelauxetic effect of 4f electrons of rare earth. On the basis of Fig. 3, the corresponding standard enthalpy of combustion and

Table 2
The standard molar enthalpies of formation of the rare earth oxide, H_2O (l) and CO_2 (g)

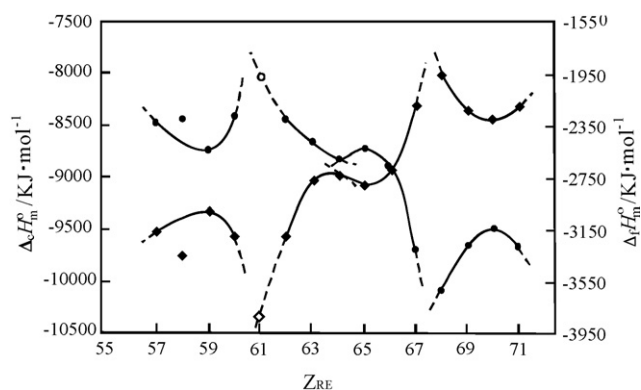| Rare earth oxide	$\Delta_f H_m^\circ$ (kJ mol^{-1})	Rare earth oxide	$\Delta_f H_m^\circ$ (kJ mol^{-1})
La$_2$O$_3$ (s)	-1791.6 ± 2.0	CeO$_2$ (s)	-1090.4 ± 1.0
Pr$_2$O$_3$ (s)	-1809.9 ± 3.0	Nd$_2$O$_3$ (s)	-1806.9 ± 3.0
Sm$_2$O$_3$ (s)	-1826.8 ± 4.8	Eu$_2$O$_3$ (s)	-1662.5 ± 6.0
Gd$_2$O$_3$ (s)	-1819.7 ± 3.6	Tb$_2$O$_3$ (s)	-1865.2 ± 6.0
Dy$_2$O$_3$ (s)	-1863.4 ± 5.0	Ho$_2$O$_3$ (s)	-1883.3 ± 8.2
Er$_2$O$_3$ (s)	-1900.1 ± 6.5	Tm$_2$O$_3$ (s)	-1889.3 ± 5.7
Yb$_2$O$_3$ (s)	-1814.5 ± 6.0	Lu$_2$O$_3$ (s)	-1877.0 ± 7.7
CO$_2$ (g)	-393.51 ± 1.3	H$_2$O (l)	-285.830 ± 4.0

Fig. 3. Plot of $\Delta_f H_m^\circ$ and $\Delta_f H^\circ_m$ values against the atomic numbers of the rare earths. (●) $\Delta_f H_m^\circ$; (◆) $\Delta_f H_m^\circ$.

the standard enthalpy of formation of Pm(HSal)$_3 \cdot$2H$_2$O could be estimated as being -8050 kJ mol^{-1} and -3800 kJ mol^{-1}, respectively.

Acknowledgements

Table 3
The constant-volume combustion energies, standard molar enthalpies of combustion and standard molar enthalpies of formation for the complexes

Complex	$\Delta_c U$ (kJ mol^{-1})	$\Delta_c H_m$ (kJ mol^{-1})	$\Delta_f H_m^\circ$ (kJ mol^{-1})
La(HSal)$_3 \cdot$2H$_2$O	-9521.64 ± 4.56	-9521.64 ± 4.56	-2353.26 ± 47.02
Ce(HSal)$_3 \cdot$2H$_2$O	-9760.57 ± 4.28	-9761.19 ± 4.28	-2308.31 ± 47.00
Pr(HSal)$_3 \cdot$2H$_2$O	-9334.09 ± 4.38	-9334.09 ± 4.38	-2544.96 ± 47.02
Nd(HSal)$_3 \cdot$2H$_2$O	-9577.31 ± 4.32	-9577.31 ± 4.32	-2305.24 ± 47.01
Sm(HSal)$_3 \cdot$2H$_2$O	-9576.67 ± 3.86	-9576.67 ± 3.86	-2315.83 ± 47.01
Eu(HSal)$_3 \cdot$H$_2$O	-9029.50 ± 3.96	-9029.50 ± 3.96	-2488.96 ± 43.82
Gd(HSal)$_3 \cdot$H$_2$O	-8978.06 ± 3.92	-8978.06 ± 3.92	-2625.06 ± 43.82
Tb(HSal)$_3 \cdot$H$_2$O	-9087.35 ± 3.84	-9087.35 ± 3.84	-2538.52 ± 43.88
Dy(HSal)$_3 \cdot$H$_2$O	-8953.87 ± 4.67	-8953.87 ± 4.67	-2671.10 ± 43.92
Ho(HSal)$_3 \cdot$H$_2$O	-8332.43 ± 4.05	-8332.43 ± 4.05	-3302.49 ± 43.98
Er(HSal)$_3 \cdot$H$_2$O	-8022.00 ± 3.84	-8022.00 ± 3.84	-3621.26 ± 43.89
Tm(HSal)$_3 \cdot$H$_2$O	-8361.32 ± 3.98	-8361.32 ± 3.98	-3276.60 ± 43.88
Yb(HSal)$_3 \cdot$H$_2$O	-8445.62 ± 3.84	-8445.62 ± 3.84	-3154.90 ± 43.88
Lu(HSal)$_3 \cdot$H$_2$O	-8343.00 ± 3.52	-8343.00 ± 3.52	-3288.77 ± 43.91

Table 4
TG data of rare earth complexes with salicylic acid

Ln	$(1/2)Ln(C_6H_4OHCOO)_3 \cdot (1/4)Ln_2O_2CO_3$[a]			$(1/3)Ln(C_6H_4OHCOO)_3 \cdot (1/3)Ln_2O_2CO_3$			$(1/2)Ln_2O_3$[b]		
	Temperature range (°C)	Residue (%)		Temperature range (°C)	Residue (%)		Temperature range (°C)	Residue (%)	
		Found	Calculated		Found	Calculated		Found	Calculated
La	25–271–304[c]	63.63	62.70	304–354–387	53.08	52.31	387–427–846	27.63	27.79
Ce	25–253–280	73.94	74.84	–	–	–	280–319–561	29.80	29.30
Pr	25–265–300	63.61	62.83	300–347–385	53.25	52.47	385–482–878	27.91	28.03
Nd	25–274–303	63.02	63.03	303–347–380	53.43	52.74	380–477–675	29.15	28.43
Sm	25–271–306	63.52	63.42	306–351–387	53.31	53.23	387–421–823	29.59	29.18
Eu	25–272–303	64.66	65.48	303–328–358	55.95	55.01	358–410–662	29.92	30.27
Gd	25–267–311	65.13	65.79	311–357–390	54.89	55.41	390–454–749	30.97	30.90
Tb	25–281–328	65.38	65.89	328–386–414	56.14	55.53	414–453–671	31.15	31.09
Dy	25–281–325	65.62	66.09	325–373–420	55.07	55.80	420–470–769	31.97	31.51
Ho	25–286–332	66.20	66.23	332–379–428	55.14	55.98	428–471–792	31.57	31.79
Er	25–285–332	66.98	66.37	332–383–428	56.01	56.16	428–463–791	32.28	32.06
Tm	25–294–348	65.93	66.46	–	–	–	348–428–793	31.93	32.24
Yb	25–308–348	67.37	66.68	–	–	–	348–407–792	32.45	32.70
Lu	25–318–355	66.02	66.79	–	–	–	355–445–792	33.22	32.93

[a] Ln = La, Pr, Nd, Sm, Eu, Gd, Tb, Dy, Ho, Er, Tm, Yb, Lu and $CeOCO_3$.
[b] Ln = La, Pr, Nd, Sm, Eu, Gd, Tb, Dy, Ho, Er, Tm, Yb, Lu and CeO_2.
[c] Intermediate temperature DTG peak temperature.

Appendix A

TG data of rare earth complexes with salicylic acid is given in Table 4.

Appendix B. Supplementary data

Supplementary data associated with this article can be found, in the online version, at doi:10.1016/j.tca.2007.07.006.

References

[1] J.P. Costes, J.M. Clemente-Juan, F. Dahan, F. Nicodam, M. Verelst, Angew. Chem. Int. Ed. 41 (2002) 323.
[2] T.M. Reineke, M. Eddaoudi, D. Kelly, O.M. Yaghi, J. Am. Chem. Soc. 121 (1999) 1651.
[3] L. Ma, O.R. Evans, B.M. Foxman, W. Lin, Inorg. Chem. 38 (1999) 5837.
[4] J.S. Seo, D. Whang, H. Lee, J.O. Jun, Y.J. Jeon, K. Kim, Nature 404 (2000) 982.
[5] S. Wang, Z. Pang, K.D.L. Smith, M.J. Wagner, J. Chem. Soc., Dalton Trans. 7 (1994) 955.
[6] Y.T. Yang, S.Y. Zhang, Spectrochim. Acta Part A 60 (2004) 2065.
[7] N. Turkel, R. Ayolin, U. Ozer, Turk. J. Chem. 23 (1999) 249.
[8] M. Marina, Anal. Chim. Acta 260 (1992) 51.
[9] M.Z. Su, G.P. Li, Chemistry 43 (1979) 34.
[10] W.J. Sun, X.W. Yang, H.G. Zhang, X.Y. Wang, S.L. Gao, J. Rare Earths 24 (2006) 423.
[11] X.W. Yang, S.P. Chen, S.L. Gao, J. Instr. Sci. Technol. 30 (2002) 311.
[12] M.M. Popov, Moscow University Publishing House, Moscow, 1954, p. 382.
[13] X.W. Yang, W.J. Sun, C.Y. Ke, L. Zhu, H.G. Zhang, S.L. Gao, Chem. Pap. 60 (2006) 132.
[14] E.H.P. Cordfunke, R.J.M. Konings, Thermochim. Acta 65 (2001) 1.
[15] J.A. Dean, Lange's Handbook of Chemistry, 15th ed., Beijing World Publishing Corporation/McGraw-Hill, Beijing, 1999, p. 6.43.